Phys. Status Solidi B **250**, No. 6, 1119–1127 (2013) / **DOI** 10.1002/pssb.201248477

Part of Special Issue on
Metal–Substrate Interactions in Heterogeneous Catalysis

physica status solidi b
www.pss-b.com
basic solid state physics

Feature Article

Covalent organic frameworks and their metal nanoparticle composites: Prospects for hydrogen storage

Suresh Babu Kalidindi and Roland A. Fischer*

Inorganic Chemistry II – Organometallics and Materials Chemistry, Faculty of Chemistry and Biochemistry, Ruhr University Bochum, 44780 Bochum, Germany

Received 9 October 2012, revised 31 January 2013, accepted 5 February 2013
Published online 11 March 2013

Keywords covalent organic frameworks, hybrid materials, hydrogen storage, metal nanoparticles, metal-organic frameworks

* Corresponding author: e-mail roland.fischer@rub.de

Covalent organic frameworks (COFs) are microporous crystalline organic frameworks with large specific surface areas. The area of COFs is rapidly developing in the direction of finding potential applications in fields like gas storage, photovoltaics, and catalysis. With respect to hydrogen storage, at first glance, COFs possess all the advantages of metal-organic frameworks (surface area, pore volume, rigidity of the structure). In addition, since the molecular frameworks of COFs are composed of light elements (C, Si, B, and O), these materials have exceptionally low densities. Due to this advantage, a lot of research activity (both theoretical and experimental) was reported in the recent literature on hydrogen-storage properties of COFs. Also, several strategies were suggested for enhancing H_2-storage capacities of COFs at cryogenic as well as room temperatures. In this feature article, we broadly discuss the scope of COFs as hydrogen storage media and also review the strategies suggested for enhanced room-temperature hydrogen-storage properties. Further, the concept of "spillover" is reviewed critically in metal@COFs and metal@MOFs systems.

1 Introduction The world's increasing energy demands, limited petroleum feed stocks and increasing greenhouse gas emissions have necessitated restructuring of our energy economy towards sustainable and renewable energy sources. In this context, hydrogen, with an energy content of 142 MJ kg^{-1} is an ideal fuel because of its environmental friendliness [1]. The concept of a hydrogen economy involves production (using renewable energy), distribution, storage, and utilization of H_2 [2]. One of the major bottlenecks for use of H_2 for onboard vehicular applications is its safe and cost-effective storage. The very low density of hydrogen in both gas (0.08 kg m^{-3} at STP) and liquid (70.8 kg m^{-3} at 20.3 K) form makes its storage a very difficult task [3]. A benchmark material should store 9 wt% of hydrogen reversibly between −30 °C to 80 °C (the 2015 target by the U.S. Department of Energy (DOE)). Also, durability of the storage material should be at least 1000 cycles and the refuel time should not exceed 3 min.

In general terms, the hydrogen-storage approaches can be divided into two types based on H_2 interaction with storage media: (i) the chemical bonding as hydrides (chemisorption), and (ii) the adsorption on surfaces (physisorption).

The chemisorbed hydrogen is difficult to remove from metal hydrides, the metal hydrides are generally too heavy as well, the only promising metal hydride is MgH_2 (7.6 wt%), which requires temperatures above 350 °C to release hydrogen [4]. On the other hand, the hydrogen physisorption process is highly reversible. However,very low temperatures are required to store significant gravimetric amounts of hydrogen.

Cryogenic hydrogen storage (typically between 60 and 120 K) have been getting immense attention, especially after the development of well-defined large surface area porous materials in particular porous coordination polymers (PCPs) or metal-organic frameworks (MOFs) [5]. Due to the weak van der Waals forces, cryoadsorption can lead to H_2 uptakes with faster kinetics. The main factors that determine H_2-storage capacity in MOFs are surface area, pore volume, and enthalpy of adsorption. The former two factors have a pronounced effect on H_2 uptakes at cryogenic temperatures, whereas the final one affects H_2 uptakes close to ambient

temperatures. It is established that H_2 uptake increases with increase in specific surface area and a linear correlation exists between the MOF BET surface area and the hydrogen uptake at 77 K. To date, the highest H_2 uptake was reported for NU-100 ($[Cu_3(ttei)(H_2O)_3]_n$; $H_6ttei = 1,3,5$-tris[(1,3-carboxylicacid-5-(4-(ethynyl) phenyl))ethynyl]-benzene), it has an excess uptake of 99.5 mg g^{-1} at 77 K and 56 bar, a value that is sufficient for practical applications [6].

Newly developed crystalline organic frameworks offer certain advantages over MOFs. The so-called covalent organic frameworks (COFs) are organic analogs of MOFs and are devoid of heavy-metal ions. COFs are constructed from functional organic building blocks by dynamic covalent formation methods [7]. These extended crystalline organic frameworks have high surface areas on a par with MOFs and low densities. Gravimetric hydrogen-storage capacity directly relates to the density of the material, therefore, COFs devoid of any heavy-metal ions will have the advantage of storing higher gravimetric amount of hydrogen due to lower density.

However, the H_2-storage capacity decreases dramatically as the temperature increases to ambient temperature, and none of the known MOFs or COFs exhibits any considerable uptake at room temperature. In this regard, the decisive factor is the enthalpy of adsorption. Theoretical calculations have shown that for significant H_2 uptake at room temperature the material should have 15–25 kJ mol^{-1} of isosteric heat of H_2 adsorption. There have also been extensive efforts to increase the isosteric heat of H_2 adsorption by introducing metal ions and metal nanoparticles on the internal surface of MOFs or COFs. In particular, metal@MOF systems are widely investigated in the context of the "spillover" phenomenon in the literature [8].

In this minireview, we will discuss the advantages and challenges with regard to COFs as hydrogen-storage media. Also, special attention will be given to metal@COFs and metal@MOFs systems with regard to room-temperature hydrogen storage.

2 Overview of existing COFs In their breakthrough work (2005), Yaghi and coworkers [9] for the first time reported solvothermal synthesis of crystalline 2D COFs, namely COF-1 and COF-5, using the topological design principle (Fig. 1). In this work, crystalline frameworks were realized by apt selection of reaction parameters. The sparing solubility of building blocks controlled the diffusion process and facilitated the nucleation of a crystalline material, and closed reaction conditions (sealed tubes) helped to maintain reversible reaction conditions by retaining the *in situ* generated water. Since this study, numerous 2D COFs have been synthesized using this approach.

Most of these COFs deal with boronic acid functionalized building blocks, because these can reversibly undergo either self-condensation or cocondensation with polyaromatic alcohols to give boroxine and boronate ester linkages, respectively. Other linkages that are used in 2D COFs include triazine, imine, and hydrazone.

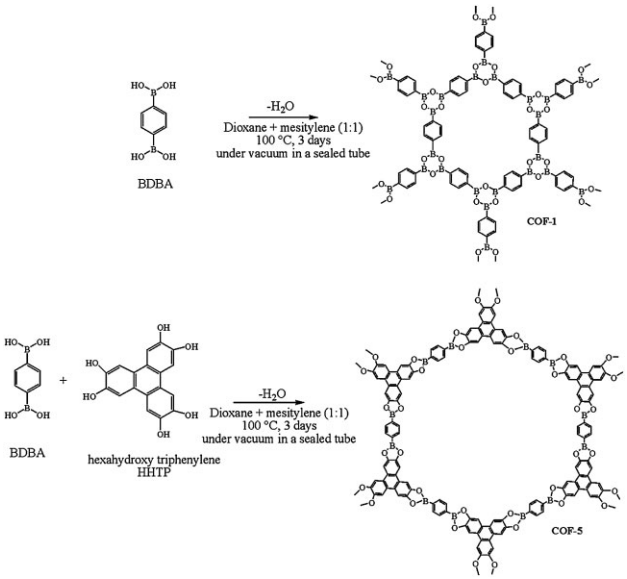

Figure 1 Synthesis of COF-1 and COF-5 from self-condensation and esterification reactions, respectively.

In 2D COFs, the π–π stacking between the layers provides uniquely ordered π systems that can increase charge-carrier transport along the axis of stacking. Therefore, 2D COFs are more appealing for optoelectronics and photovoltaics applications rather than gas-storage applications. On the other hand, 3D COFs have very high surface areas compared to 2D COFs and are more known for their gas-storage properties.

The 3D COFs have been synthesized from tetrahedral nodes or by using appropriate combinations of tetrahedral and triangular nodes [10]. 3D COFs based on boroxine (COF-102, COF-103), boronate ester (COF-105, COF-108), borosilicate (COF-202), and imine (COF-300) linkages are known. The boroxine based COF-102 (Fig. 2), and COF-103

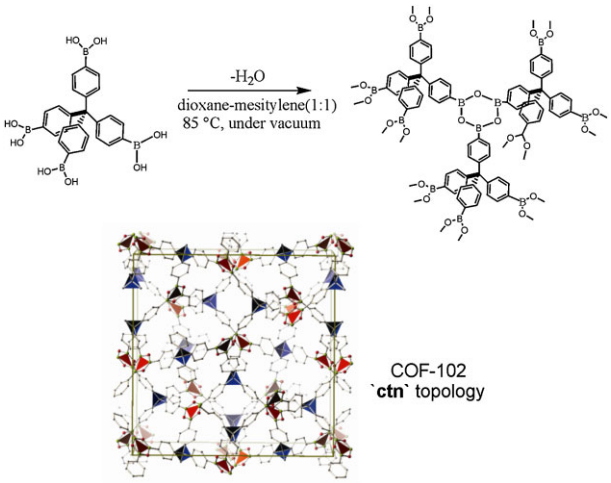

Figure 2 (online color at: www.pss-b.com) Synthesis and topology of COF-102.

have been synthesized by self-cocondensation of tetrahedral nodes, namely, tetra(4-dihydroxyborylphenyl)methane (TBPM), and tetra(4-dihydroxyborylphenyl)silane (TBPS), respectively. Both of these materials adopt **ctn** topology. The boronate ester based COF-105, COF-108 have been obtained by the condensation of tetrahedral node TBPM and triangular node 2,3,6,7,10,11-hexahydroxy triphenylene (HHTP) in different molar ratios. COF-105 and COF-108 have **ctn** and **bor** topologies, respectively. Condensation of tert-butylsilane triol and TBPM in 1:2 v/v dioxane/toluene solvent mixture led to the formation of COF-202 that adopted a **ctn** network. The imine-based COF-300 has interesting multiply interpenetrated **dia-c5** structure and was obtained by the condensation of the tetrahedral building block tetra-(4-anilyl)methane with the linear linking unit terephthaldehyde.

These 3D COFs have high surface areas (up to $4000\,m^2\,g^{-1}$) and lower mass densities. The surface areas, pore volumes and densities of 3D COFs are summarized in Table 1. The lower density values are extremely advantageous for hydrogen storage.

3. Hydrogen storage in COFs

3.1 Cryogenic storage Cryoadsorption (60–120 K) is mainly governed by van der Waals forces and is highly reversible. The only drawback is that the maintenance of cryotanks on vehicles is an energy-intensive process and is not economical.

3.1.1 Theoretical investigations The potential applications of COFs for hydrogen storage were initially evaluated using a wide range of sophisticated multiscale theoretical protocols. Most of these studies predicted superior gravimetric H_2 uptake for 3D COFs at 77 K when compared to high surface area MOFs.

Froudakis and coworkers [11] used density functional theory (DFT) and second-order Møller–Plesset perturbation theory (MP2) calculations to obtain hydrogen binding sites and the interaction potential curves. The studies revealed that most favorable sites for H_2 adsorption are phenyl rings and B_3O_3 or C_2BO rings with binding energies $<1\,kcal\,mol^{-1}$.

Molecular dynamic (MD) simulations carried out by Assfour and Seifert [12] are also consistent with these binding energy values. The observed binding energy values are comparable with those calculated in previous studies for IRMOFs. The binding energies are too small to play any role in the H_2 volumetric uptake. In other words, for comparable surface areas, COFs and MOFs store similar volumetric amounts of hydrogen. However, greater gravimetric capacity can be expected for COFs due to the lower density. The H_2 isotherms obtained using grand canonical Monte Carlo (GCMC) simulations have shown that this is indeed the case [13]. The calculated total gravimetric uptake of COF-108 (density: $0.17\,g\,cm^{-3}$) at 100 bar is 21 wt% at 77 K and a very attractive 4.5 wt% at room temperature (300 K).

Yaghi and coworkers [14] reported GCMC simulations on both 2D and 3D COFs. In these studies, more accurate *ab initio* parameters were obtained by using force fields (FF) derived from *ab initio* second-order Møller–Plesset (MP2) calculations using quadruple-ζQZVPP basis set and basis set superposition error correction. As expected, 3D COFs have shown 2–3 times higher hydrogen-storage capacity than 2D COFs due to high surface area and free volume (Fig. 3). The perfect correlation between experimental and theoretical results was shown in the case of COF-5. All these theoretical studies have shown that to increase H_2 gravimetric storage capacity of COFs both surface area and free volume should be increased.

Froudakis and coworkers [15] proposed novel 3D COFs for enhanced hydrogen-storage capacity. These structures were derived from COF-102 by substituting phenyls rings of TBPM with various aromatic moieties without **ctn**. Replacement with diphenyl, triphenyl, napthalene, and pyrene molecules produced COF-102-2, COF-102-3, COF-102-4, and COF-102-5, respectively (Fig. 4). All the structures were optimized using the MM3 FF. The MM3 FF was parameterized for COF-102 on the basis of first-principles calculations of non-periodic model systems [16]. Classical GCMC simulations were used to obtain the total gravimetric and volumetric uptake at 77 and 300 K from the optimized structures. Among the four proposed 3D COFs, COF-102-3 showed the best gravimetric storage capacities: 26.7 and

Table 1 Overview of 3D COFs known so far.

COF	ligands	linkage	topology	BET surface area ($m^2\,g^{-1}$)	pore volume ($cm^3\,g^{-1}$)	density ($g\,cm^{-3}$)
COF-102	tetra(4-dihydroxyborylphenyl)methane	boroxine	**ctn**	3472	1.35	0.41
COF-103	tetra(4-dihydroxyborylphenyl)silane	boroxine	**ctn**	4210	1.66	0.38
COF-105	tetra(4-dihydroxyborylphenyl)methane and 2,3,6,7,10,11-hexahydroxy triphenylene	boronate ester	**ctn**	–	–	0.18
COF-108	tetra(4-dihydroxyborylphenyl)methane and 2,3,6,7,10,11-hexahydroxy triphenylene	boronate ester	**bor**	4700	–	0.17
COF-202	tetra(4-dihydroxyborylphenyl)methane and tert-butylsilane triol	borosilicate	**ctn**	2690	1.09	–
COF-300	tetra-(4-anilyl)methane and terephthaldehyde	imine	**dia**	1360	0.72	0.54

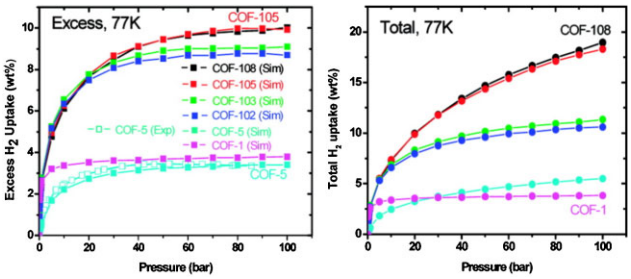

Figure 3 (online color at: www.pss-b.com) Excess and total H_2 isotherms at 77 K for various 2D and 3D COFs. Filled and open symbols represent simulation and experimental results for COF-5, respectively. Reprinted with permission from Ref. [14], Copyright (2008) American Chemical Society.

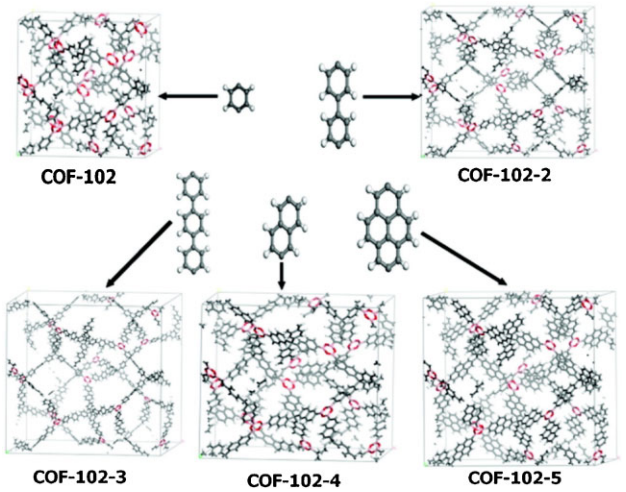

Figure 4 (online color at: www.pss-b.com) Construction of COF-102-2, COF-102-3, COF-102-4, and COF-102-5 by using COF-102 connectivity and topology. Reprinted with permission from Ref. [15], Copyright (2008) American Chemical Society.

6.5 wt% at 77 and 300 K, respectively, at 100 bar. However, these materials showed lower volumetric performance than the parent COF-102. For example, COF-102-3 has volumetric capacity of $\sim$35 g L^{-1} compared to $\sim$42 g L^{-1} for COF-102 at 77 K and 100 bar. It should be noted that very large pores inside the material result in empty space that is dominated by weak fluid–fluid interactions. This in turn decreases volumetric capacity. The pore volume and surface area should be balanced to achieve optimized gravimetric and volumetric storage capacities.

Recently, pillaring of COF-1 with pyridine has been shown to enhance both gravimetric and volumetric hydrogen uptake at 77 K [17]. Pyridine molecules bound to the boron atoms of a B_3O_3 ring can generate semi-3D structures (pillared COFs) with large surface area. Three structural isomers (two eclipsed and one staggered) were optimized using DFT calculations and respective H_2 isotherms were obtained using GCMC simulations. The calculations have shown that the pyridine pillars not only increase the interlayer spacing but also create additional hydrogen-adsorption sites. As a result, the gravimetric storage capacity can be improved up to 10 wt% and volumetric capacity up to 60 g L^{-1} from 3.6 wt% and 37.6 g L^{-1}, respectively. These results emphasize the importance of effective utilization of free volume.

3.1.2 Experimental investigations Furukawa and Yaghi [18] studied the hydrogen-storage properties of various 2D COFs and 3D COFs at 77 K. The saturation uptakes of 2D COFs are: 15 mg g^{-1} for COF-1, 36 mg g^{-1} for COF-5, 23 mg g^{-1} for COF-6, 35 mg g^{-1} for COF-8, and 39 mg g^{-1} for COF-10. 3D COFs outperformed 2D COFs and the saturation uptake values are: 72.4 mg g^{-1} for COF-102 and 70.5 mg g^{-1} for COF-103. These uptakes are significant and demonstrate the potential of COFs as hydrogen-storage materials. It is noteworthy that the H_2 uptake of COF-102 is comparable with that of MOF-177 (75 mg g^{-1}) and MOF-5 (76 mg g^{-1}). Even though other 3D COFs, COF-105, and COF-108 have been predicted to show higher H_2 uptakes, experimental values are not available in the literature. This could be due to the problems associated with the activation of these materials.

The experimental H_2-uptake values of various COFs suggest almost linear increase in gravimetric uptake with increase in specific surface area (Fig. 5). This again reinforces the fact that H_2-COF surface interactions are negligible under cryogenic conditions and H_2 uptakes are independent of the composition of the structure's backbone.

The coverage dependency of adsorption enthalpies of various COFs is shown in Fig. 6. COF-1 has the highest isosteric heat of adsorption (Q_{st}) and the value decreases almost linearly with increase H_2 in coverage. 3D COFs have very low Q_{st} values over the whole range of coverage measured.

3.2 Room-temperature storage As it evident from the above discussion, COFs are attractive hydrogen-storage

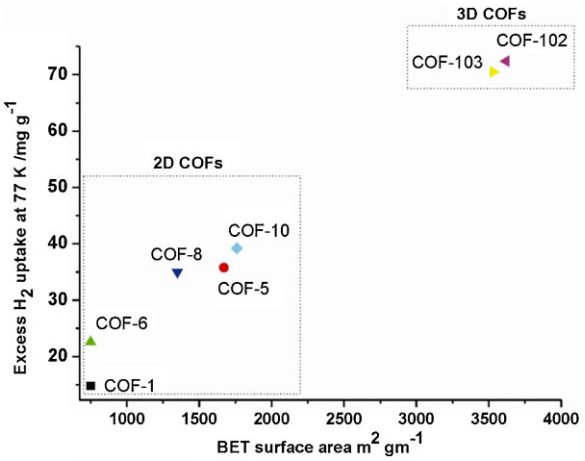

Figure 5 (online color at: www.pss-b.com) Excess hydrogen uptake at 77 K versus BET specific surface area for various 2D and 3D COFs.

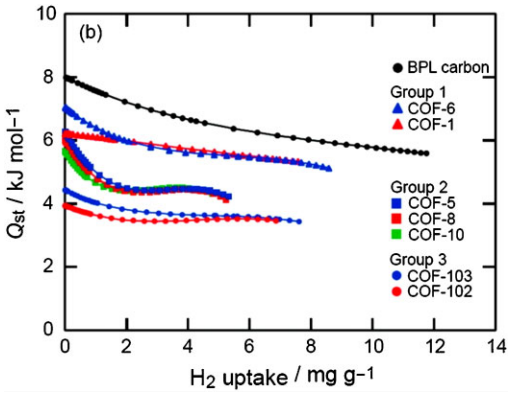

Figure 6 (online color at: www.pss-b.com) Coverage dependency of adsorption enthalpies for various 2D and 3D COFs. Data for BPL carbon are shown for comparison. Reprinted with permission from Ref. [18], Copyright (2008) American Chemical Society.

materials at low temperatures. However, their H_2-storage capacities under ambient conditions are still low and cannot meet the DOE targets. Neat COF surfaces have weak interaction energies with H_2 molecules. The observed Q_{st} values (7–4 kJ mol^{-1}) are far too low compared to benchmark values of 15–25 kJ mol^{-1} for room-temperature storage. In the case of MOFs, it was suggested that room-temperature storage capacities could be increased by decorating the surfaces with positively charged metal ions or with metal nanoparticles [19]. Similar strategies were also considered in the case of COFs.

3.2.1 Theoretical studies Cao et al. [20] studied Li-doped 3D COFs for room temperature H_2 storage using first-principles calculations and GCMC simulations. The distribution and charge on the Li plays a crucial role in determining H_2 interaction energies. In these calculations, eight Li atoms are placed TBPM or TBPS building blocks and one lithium atom on HHTP ligand. Agglomeration of Li atoms into the clusters can inhibit the charge transfer from Li to COFs. Therefore, the Li distribution is the decisive factor in determining H_2 adsorption enthalpies. Also, it was assumed that lithium atoms are positively charged on the COF surface and the charges transferred from Li atoms to the COFs are in the range from 0.3 to 0.5 |e| per Li atom. When the H_2 molecule comes close to a positively charged Li atom, the electron density is transferred from the H_2 molecule to the Li atom. A dative bond will be formed between the 2s orbital of Li atom and the H_2 σ bond [21]. The strong affinity of the positively charged Li atom for H_2 is essentially governed by charge-induced dipole and charge–quadrupole interactions.

The calculated isosteric heats of hydrogen in the Li-doped COFs are evidently larger. The calculated maximum isosteric heats of H_2 in Li-doped 3D COFs at $T = 298$ K are: 22.99 kJ mol^{-1} for COF-102, 23.66 kJ mol^{-1} for COF-103, 21.88 kJ mol^{-1} for COF-105, and 20.09 kJ mol^{-1} for COF-108. The values are approximately 4–5 times higher when compared to neat surfaces. The gravimetric H_2 uptakes for Li-doped COF-105 and COF-108 are 6.84 and 6.73 wt%, respectively, at $T = 298$ K and $p = 100$ bar. These values are very promising and reinforce the necessity of the presence of strong interaction sites on the COF surface for H_2 storage under ambient conditions.

Kang and coworkers [22] also studied the doping effect of Li^+, Mg^{2+}, and Ti on room-temperature hydrogen-storage capacities of 3D COFs using second-order Møller–Plesset perturbation theory (MP2). The results suggested Li^+- and Mg^{2+}-decorated COF-108s can store 6.5 and 6.8 wt% of H_2 at room temperature, respectively.

Functionalization of linkers was also suggested to increase H_2-storage capacities at room temperature [23]. Lithium alkoxide groups were introduced into COF-105 by adding three lithium alkoxide groups per HHTP building unit. The GCMC simulation studies on DFT optimized structures showed that 6 wt% H_2 gravimetric storage capacities can be obtained. The calculated H_2 interaction energy with Li is 12.3 kJ mol^{-1}, a value that is almost three times larger than the interaction of H_2 with neat COF-105 surface.

Recently, using quantum-mechanical (QM) methods, it was shown that $PdCl_2$ incorporated COF-301 stores 60 g L^{-1} (4.2 wt% excess) H_2 at 100 bar, which is 1.5 times the DOE 2015 target of 40 g L^{-1} (Fig. 7) [24]. The incorporation of $PdCl_2$ inside COF-301 reduced the surface area from 3700 to 1080 m^2 g^{-1} and the pore volume from 1.08 to 0.42 cm^3 g^{-1}. However, the observed higher H_2 uptakes are due to the high interaction energy between the Pd site and H_2. The Q_{st} value was found to be 23 kJ mol^{-1} versus 6 kJ mol^{-1} for an unmodified COF-301 surface. Even though Pd complexation inside COF-301 was found to be favorable theoretically, attempts to make such compound are unsuccessful. This could be due to the problems associated with $PdCl_2$ diffusion into COF-301 pores.

3.2.2 Experimental studies Even though several theoretical studies predict that surface-modified COFs or MOFs can act as excellent candidates for room-temperature hydrogen storage, till now most of these strategies have not been demonstrated experimentally. This is mainly due to the experimental difficulties involved in the synthesizing suggested modified COFs or MOFs.

One concept that is widely studied experimentally in both MOFs and COFs with regard to room-temperature hydrogen storage is spillover. Spillover can be defined as the

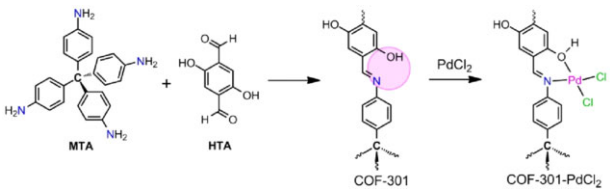

Figure 7 (online color at: www.pss-b.com) Proposed scheme for the synthesis of COF-301-$PdCl_2$. Reprinted with permission from Ref. [24], Copyright (2012) American Chemical Society.

dissociative chemisorption of H_2 molecules on a metal catalyst, followed by migration of monatomic hydrogen (somehow) into the porosity of the host MOF or COF.

Metal-combined MOF/COFs systems are found to exhibit very attractive H_2-storage capacities at room temperature [25]. It was found that when MOFs or COFs are combined with transition-metal catalysts such as Pt/C, the H_2 uptakes can be increased up to six- to sevenfold, due to the spillover process. Here, activated carbon acts as a primary spillover source and the MOF/COF as a secondary spillover source (Fig. 8a). The contact between primary and secondary spillover sources plays a major role in deciding the overall H_2 uptakes. The contact can be increased by building a carbon bridge by carbonization of a hydrocarbon precursor such as sucrose. Li and Yang [25] reported that by using a bridge technique, in the case of IRMOF-8 the H_2 uptake at room temperature can be increased from 0.5 wt% (for pristine MOF) to 4 wt% at 10 MPa pressure.

Other kinds of metal/MOF systems studied for the spillover process include metal-nanoparticle-decorated MOFs (Fig. 8b, metal@MOF). The synthesis and properties of metal@MOFs materials were recently reviewed by Fischer and coworkers [8]. In these systems, the metal nanoparticles are in direct contact with MOFs and are present either in the pores or the surface of MOFs. Hence, MOFs act as primary spillover sources. However, unexpectedly the H_2 capacities reported in these systems are much lower than the reported for former systems where the MOF acts as a secondary bridge.

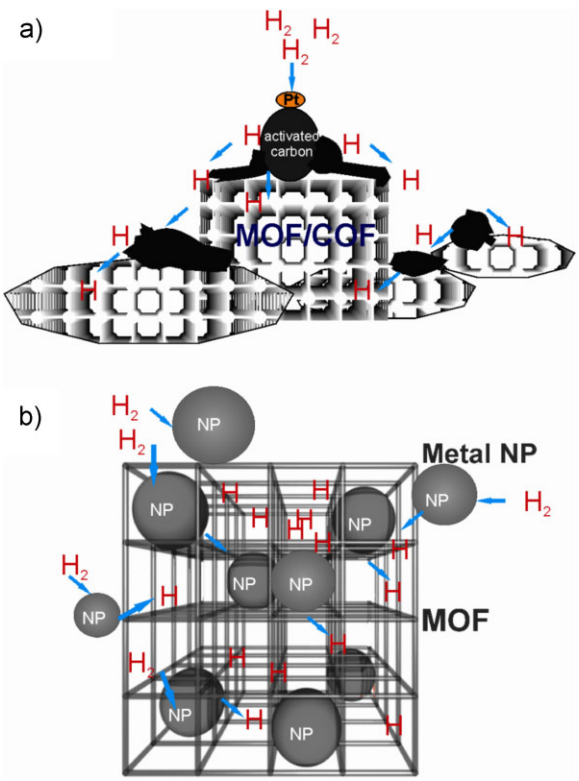

Figure 8 (online color at: www.pss-b.com) Proposed spillover concept in (a) bridged metal/AC/MOF system; (b) metal NPs@MOF systems.

Investigations of the hydrogen-adsorption properties of 3 wt%PdNPs@$[SNU\text{-}3]^{0.54+}(NO_3^-)_{0.54}$ (SNU-3 = $[Zn_3(ntb)_2]_n$, ntb = 4,4′,4″-nitrilotrisbenzoate) have shown an uptake of 0.30 wt% versus 0.13 wt% for pristine SNU-3 at 298 K and 95 bar [26]. Surprisingly, in these studies the H_2 uptake at 77 K was also found to increase after Pd impregnation even though there is a huge drop in N_2 uptake. The H_2 uptake at 77 K increased to 1.48 wt% at 1 atm, compared to 1.03 wt% for pristine SNU-3. Making things more complex, it was also found that the zero-coverage isosteric heat of adsorption is lower for PdNPs@$[SNU\text{-}3]^{0.54+}(NO_3^-)_{0.54}$ (6.62 kJ mol^{-1}) compared to pristine SNU-3(8.11 kJ mol^{-1}). The unexplainable higher uptakes were assigned to spillover process. But the spillover process at 77 K is elusive.

On the other hand, Latroche and coworkers [27] reported that H_2 uptake at 77 K in 10 wt% Pd@MIL-100(Al) decreased to 1.3 wt% from 3.1 wt% for pristine MIL-100(Al) and this was ascribed to the textural changes induced by Pd insertion. However, at room temperature the excess hydrogen uptake was almost doubled for Pd@MIL-100(Al) (0.35 wt% at 4 MPa versus 0.19 wt% for pristine MIL-100(Al)). Again, this enhancement was attributed to the spillover process.

The only report that deals with COFs and spillover is that of Li and Yang [28]. The room-temperature H_2 uptake of COF-1 can be increased 2- to 3.5-fold by using the spillover technique. In these experiments, 5 wt% Pt on activated carbon was used as a catalyst for H_2 dissociation.

As is evident from the above discussion in most cases, to explain the elusive H_2 uptake enhancements observed in the case of complex hybrid materials the spillover process is used. However, so far there is no concrete evidence to prove the spillover phenomenon in metal/MOF or metal@MOF systems. Even though the spillover phenomenon is widely accepted in the area of catalysis, this topic remains one of the most debatable topics in the area of hydrogen storage [29]. This is due to the lack of direct evidence for the migration of H atoms into the pores of MOFs. The atomic hydrogen produced by the noble-metal catalysts after dissociative chemisorption of H_2 molecules will be highly reactive and try to form chemical bonds or recombine to hydrogen molecules. This could make H_2 adsorption phenomenon non-reversible. For example, the spillover studies on Pt@MOF-177 revealed that the H_2 uptake is not reversible [30]. For the first cycle, at room temperature the H_2 adsorption is almost 2.5 wt%, but is decreased to 0.5 wt% (almost equal to pristine MOF) in consecutive cycles.

Moreover, there exists a discrepancy in the literature (Fig. 9) in reproducing some of the results [31]. In this backdrop, the concept of spillover does not seem to be a very reliable method to increase H_2 uptakes in systems such as metal/MOF or metal/COFs.

In this context, Fischer and coworkers [32] recently reported hydrogen properties of Pd@COF-102 hybrid material. Initially, the Pd-(η^3-C_3H_5(η^5-C_5H_5)]@COF-102

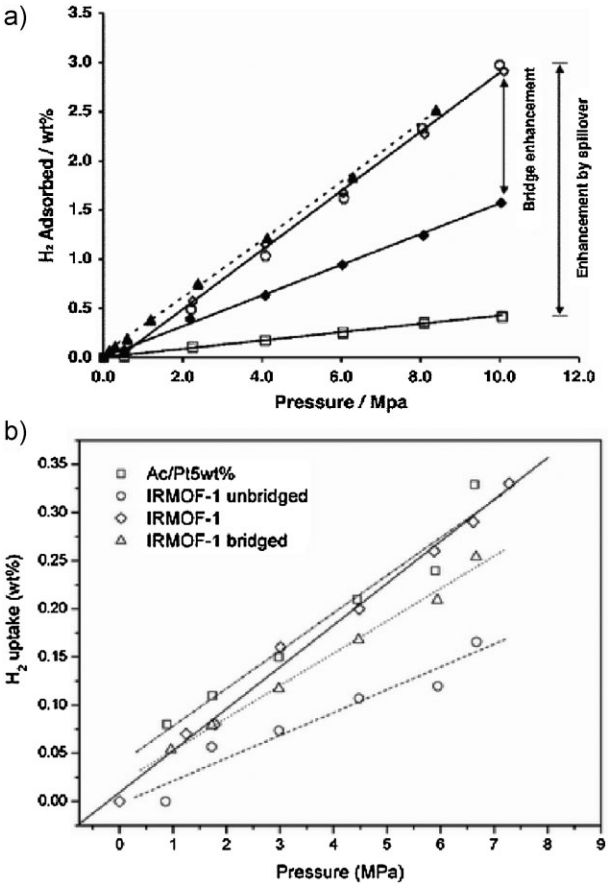

Figure 9 Hydrogen adsorption isotherms of IRMOF-1 composites, at RT: (a) by Li and Yang. Reprinted with permission from Ref. [25], Copyright (2006) American Chemical Society; (b) by Hirscher and coworkers. Reprinted with permission from Phys. Chem. Chem. Phys. **12**, 10457 (2010) [31], Copyright (2010), The Royal Society of Chemistry. Even though sample preparation methods and experimental techniques used in both papers are very much similar, the effect of Pt/AC in both cases is very different.

inclusion compound is synthesized by a gas-phase infiltration method. The solvent-free gas-phase infiltration technique is widely employed for the synthesis of metal@MOF systems [33]. This method allows high and uniform loadings of metal nanoparticles into the pores of MOFs or COFs. The decomposition of the inclusion compound in the presence of UV light resulted in the formation of highly monodispersed nanoparticles with an average particle size of 2.4 ± 0.5 nm (Fig. 10). The Pd nanoparticles were homogeneously distributed thorough out the COF-102 crystals and this was established using the electron tomography method (Fig. 10). Also, any detectable destruction of the framework was not noticed by powder XRD and NMR techniques, after incorporation of Pd nanoparticles inside COF-102.

At 77 K, the hydrogen uptake decreased to 4.6 wt% from 5.3 wt% after Pd nanoparticle loading. This is due to the decrease of the specific surface area and pore volume after Pd loading. The hydrogen storage studies at room temperature show that H_2 uptakes were enhanced by a factor of 2–3 after

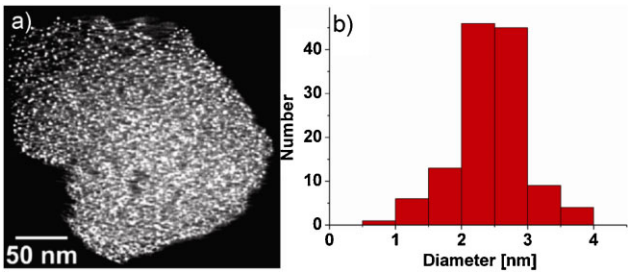

Figure 10 (online color at: www.pss-b.com) (a) Orthoslice through the 3D reconstruction of heavily loaded Pd@COF-102 hybrid crystal; (b) size distribution of Pd nanoparticles. Reproduced from Ref. [32].

Pd incorporation inside the COF-102 pores. However, in this case, the enhanced uptakes were assigned to Pd hydride formation and hydrogenation of residual organics present on the Pd nanoparticle surface, rather than spillover (Fig. 11). The residual organics come from the precursor [Pd-(η^3-C_3H_5(η^5-C_5H_5)]. The evidence for the presence of bycyclopentadiene on the surface of Pd nanoparticles was obtained from IR, NMR, and thermal desorption spectroscopy techniques. This study demonstrates the need for thorough characterization of materials to ascertain reasons for enhanced H_2 uptakes observed in hybrid materials containing several components.

The spillover process in the context of hydrogen storage is also reported in systems where metal nanoparticles are stabilized using noncrystalline porous organic polymers. For example, Pd nanoparticles dispersed throughout a microporous poly-(aryleneethynylene) material enhances H_2 uptake from 0.006 to 0.069 wt% for 9.5 wt% of Pd content [34]. Similarly, Liang and coworkers [35] reported an enhancement factor of 1.75 for a Pt@(pentaerythritol tetrakis 3-mercaptopropionate)-poly(vinylbenzyl chloride) polymer system. Even though the H_2-uptake values are far less than their crystalline counterparts (MOF or COFs), these compounds are more robust.

4 Conclusions and perspective remarks In summary, undoubtedly COFs are potential candidates for H_2 storage due to well-defined structures, high surface areas,

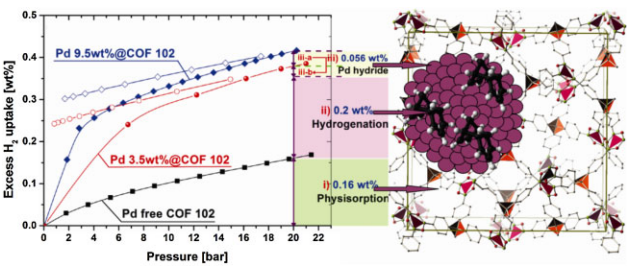

Figure 11 (online color at: www.pss-b.com) Left: Excess H_2 sorption isotherms of Pd@COF-102 sample; Right: Pictorial representation of Pd nanoparticles inside COF-102. Contribution of various factors towards enhanced H_2 storage is also shown. Reproduced from Ref. [32].

and high pore volumes, especially for cryogenic H_2 storage. For instance, COF-102 stores 7.2 wt% of H_2 at 77 K, which is close to the 2015 DOE target. More attractive H_2-storage capacities were reported theoretically with 3D COFs such as COF-105 and COF-108. However, no experimental studies are reported on these COFs owing to problems associated with pore activation. Such experimental difficulties need to be overcome for further exploration of the hydrogen-storage properties of COFs.

Regarding room-temperature storage, as is evident from the above discussion the spillover technique does not seem to be a reliable way to increase H_2 uptakes in systems such as metal@MOF or meta@COFs. Even though the results obtained in the case of organics combined Pd@COF-102 hybrid material are encouraging, the advancement is far less for practical applications. Alkali-metal doping is the most attractive prospect for room-temperature storage, however, the structural stability and extent of alkali-metal dispersion still needs to be tested.

The structural variations available in COF are also very much limited. Functionalized COFs are yet to be reported. Finally, the stability of COFs towards water also needs to be improved for practical applications. Further progress in this area will depend greatly on how COF synthetic chemistry advances in the future.

With regard to stability, use of robust porous organic polymers is an interesting prospect. Recent synthetic developments in the area of porous organic polymers have made it possible to achieve very high surface areas even in case of non-crystalline materials [36]. For instance, porous aromatic framework-1(PAF-1) synthesized from the condensation of tetrakis(4-bromophenyl)methane possesses very high BET surface area of 5640 $m^2 g^{-1}$ [37]. PAFs are highly stable and can be used under ambient conditions without degradation. Metal@PAF systems could be potential materials for room-temperature H_2 storage.

Acknowledgements SBK is grateful to the Alexander von Humboldt foundation for a fellowship.

References

[1] A. W. C. van den Berg and C. O. Areán, Chem. Commun., 668 (2008).
[2] S. Pacala, and R. Socolow, Science **305**, 968 (2004); P. Grant, Nature **424**, 129 (2003); M. S. Dresselhaus, and I. L. Thomas, Nature **414**, 332 (2001); J. A. Turner, Science **305**, 972 (2004); E. A. Fletcher, and R. L. Moen, Science **197**, 1050 (1977); A. Steinfeld, Int. J. Hydrogen Energy **27**, 611 (2002); J. Funk, Int. J. Hydrogen Energy **26**, 185 (2001).
[3] L. Schlapbach and A. Züttel, Nature **414**, 353 (2001).
[4] B. Bogdanović, A. Ritter, and B. Spliethoff, Angew. Chem. Int. Ed. **29**, 223 (1990); B. Peng, J. Liang, Z. Tao, and J. Chen, J. Mater. Chem. **19**, 2877 (2009); B. Sakintuna, F. Lamari-Darkrimb, and M. Hirscher, Int. J. Hydrogen Energy **32**, 1121 (2007).
[5] M. Hirscher, Angew. Chem. Int. Ed. **50**, 581 (2011).
[6] O. K. Farha, A. O. Yazaydin, I. Eryazici, C. D. Malliakas, B. G. Hauser, M. G. Kanatzidis, S. T. Nguyen, R. Q. Snurr, and J. T. Hupp, Nature Chem. **2**, 944 (2010).
[7] X. Feng, X. Ding, and D. Jiang, Chem. Soc. Rev. **41**, 6010 (2012).
[8] M. P. Suh, H. J. Park, T. K. Prasad, and D.-W. Lim, Chem. Rev. **112**, 782 (2012); M. Meilikhov, K. Yusenko, D. Esken, S. Turner, G. Van Tendeloo, and R. A. Fischer, Eur. J. Inorg. Chem. 3701, (2010).
[9] A. P. Côté, A. I. Benin, N. W. Ockwig, M. O'Keeffe, A. J. Matzger, and O. M. Yaghi, Science **310**, 1166 (2005).
[10] H. M. El-Kaderi, J. R. Hunt, J. L. Mendoza-Cortés, A. P. Côté, R. E. Taylor, M. M. O'Keeffe, and O. M. Yaghi, Science **316**, 268 (2007); J. R. Hunt, C. J. Doonan, J. D. LeVangie, A. P. Cote, and O. M. Yaghi, J. Am. Chem. Soc. **130**, 11872 (2008); F. J. Uribe-Romo, J. R. Hunt, H. Furukawa, C. Klock, M. O'Keeffe, and O. M. Yaghi, J. Am. Chem. Soc. **131**, 4570 (2009).
[11] E. Klontzas, E. Tylianakis, and G. E. Froudakis, J. Phys. Chem. C **112**, 9095 (2008).
[12] B. Assfour and G. Seifert, Chem. Phys. Lett. **489**, 86 (2010).
[13] G. Garberoglio, Langmuir **23**, 12154 (2007).
[14] S. S. Han, H. Furukawa, O. M. Yaghi, and W. A. Goddard, J. Am. Chem. Soc. **130**, 11580 (2008).
[15] E. Klontzas, E. Tylianakis, and G. E. Froudakis, Nano Lett. **10**, 452 (2010).
[16] R. Schmid and M. Tafipolsky, J. Am. Chem. Soc. **130**, 12600 (2008).
[17] D. Kim, D. H. Jung, K.-H. Kim, H. Guk, S. S. Han, K. Choi, and S.-H. Choi, J. Phys. Chem. C **116**, 1479 (2012).
[18] H. Furukawa and O. M. Yaghi, J. Am. Chem. Soc. **131**, 8875 (2009).
[19] K. L. Mulfort and J. T. Hupp, J. Am. Chem. Soc. **129**, 9604 (2007); S. S. Han and W. A. Goddard, J. Am. Chem. Soc. **129**, 8422 (2007); Y. E. Cheon and M. P. Suh, Angew. Chem. Int. Ed. **48**, 2899 (2009).
[20] D. Cao, J. Lan, W. Wang, and B. Smit Angew. Chem. Int. Ed. **48**, 4730 (2009).
[21] A. Mavrandonakis, E. Tylianakis, A. K. Stubos, and G. E. Froudakis, J. Phys. Chem. C **112**, 7290 (2008); J. G. Vitillo, A. Damin, A. Zecchina, and G. Ricchiardi, J. Chem. Phys. **122**, 114311 (2005).
[22] Y. J. Choi, J. W. Lee, J. H. Choi, and J. K. Kang, Appl. Phys. Lett. **92**, 173102 (2008).
[23] E. Klontzas, E. Tylianakis, and G. E. Froudakis, J. Phys. Chem. C **113**, 21253 (2009).
[24] J. L. Mendoza-Cortes, W. A. Goddard, III, H. Furukawa, and O. M. Yaghi, J. Phys. Chem. Lett. **3**, 2671 (2012).
[25] Y. W. Li and R. T. Yang, J. Am. Chem. Soc. **128**, 726 (2006); J. Am. Chem. Soc. **128**, 8136 (2006).
[26] Y. E. Cheon and M. P. Suh, Angew. Chem. Int. Ed. **48**, 2899 (2009).
[27] C. Zlotea, R. Campesi, F. Cuevas, E. Leroy, P. Dibandjo, C. Volkringer, T. Loiseau, F. Férey, and M. Latroche, J. Am. Chem. Soc. **132**, 2991 (2010).
[28] Y. Li and R. T. Yang, AIChE J. **54**, 269 (2007).
[29] C. Zandonella, Nature **410**, 734 (2001); M. Hirscher, M. Becher, M. Haluska, U. Dettlaff-Weglikowska, A. Quintel, G. S. Duesberg, Y.-M. Choi, P. Downes, M. Hulman, S. Roth, I. Stepanek, and P. Bernier, Appl. Phys. A **72**, 129 (2001).

[30] S. Proch, J. Herrmannsdörfer, R. Kempe, C. Kern, A. Jess, L. Seyfarth, and J. Senker, Chem. Eur. J. **14**, 8204 (2008).
[31] R. Campesi, F. Cuevas, M. Latroche, and M. Hirscher, Phys. Chem. Chem. Phys. **12**, 10457 (2010); S. M. Luzan and A. V. Talyzin, Micropor. Mesopor. Mater. **135**, 201 (2010); M. Hirscher, Micropor. Mesopor. Mater. **135**, 209 (2010).
[32] S. B. Kalidindi, H. Oh, M. Hirscher, D. Esken, C. Wiktor, S. Turner, G. V. Tendeloo, and R. A. Fischer, Chem. Eur. J. **18**, 10848 (2012).
[33] S. Hermes, M.-K. Schröter, R. Schmid, L. Khodeir, M. Muhler, A. Tissler, R. W. Fischer, and R. A. Fischer, Angew. Chem. Int. Ed. **44**, 6237 (2005); D. Esken, X. Zhang, O. I. Lebedev, F. Schröder, and R. A. Fischer, J. Mater. Chem. **19**, 1314 (2009); M. Müller, O. I. Lebedev, and R. A. Fischer, J. Mater. Chem. **18**, 5274 (2008); F. Schröder, D. Esken, M. Cokoja, M. W. E. van den Berg, O. I. Lebedev, G. Van Tendeloo, B. Walaszek, G. Buntkovsky, H.-H. Limbach, B. Chaudret, and R. A. Fischer, J. Am. Chem. Soc. **130**, 6119 (2008); M. Müller, S. Hermes, K. Kähler, M. W. E. van den Berg, M. Muhler, and R. A. Fischer, Chem. Mater. **20**, 4576 (2008).
[34] T. Hasell, C. D. Wood, R. Clowes, J. T. A. Jones, Y. Z. Khimyak, D. J. Adams, and A. I. Cooper, Chem. Mater. **22**, 557 (2010).
[35] B. Li, X. Huang, R. Gong, M. Ma, X. Yang, L. Liang, and B. Tan, Int. J. Hydrogen Energy **37**, 12813 (2012).
[36] T. Benb and S. Qiu, Cryst. Eng. Comm. **15**, 17 (2013).
[37] T. Ben, H. Ren, S. Ma, D. Cao, J. Lan, X. Jing, W. Wang, J. Xu, F. Deng, J. M. Simmons, S. Qiu, and G. Zhu, Angew. Chem. Int. Ed. **48**, 9457 (2009).